Title
Development and Verification of a Numerical Technique for Coupled Hyd romechanical Phenomena in Rocks

Authors
Noorishad, J.
Tsang, C.F.

Publication Date
1990-06-01

LBL-30751
UC-403

Lawrence Berkeley Laboratory
UNIVERSITY OF CALIFORNIA

EARTH SCIENCES DIVISION

Presented at the ISRM Conference on Rock Joints,
Loen, Norway, June 4–6, 1990, and to be published
in the Proceedings

Development and Verification of a Numerical Technique for Coupled Hydromechanical Phenomena in Rocks

J. Noorishad and C.F. Tsang

June 1990

Prepared for the U.S. Department of Energy under Contract Number DE-AC03-76SF00098

DISCLAIMER

LBL-30751

Development and Verification of a Numerical Technique for Coupled Hydromechanical Phenomena in Rocks

J. Noorishad and C.F. Tsang

Earth Sciences Division
Lawrence Berkeley Laboratory
University of California
Berkeley, CA 94720

This work was supported in part by a grant from the Swedish Nuclear Power Inspectorate (SKI), Stockholm, Sweden and by the Office of Energy Research, Office of Basic Energy Sciences, Engineering and Geoscience Division of the U.S. Department of Energy under Contract No. DE-AC03-76SF00098.

Development and verification of a numerical technique for coupled hydromechanical phenomena in rocks

J. NOORISHAD AND C. F. TSANG
Earth Sciences Division
Lawrence Berkeley Laboratory
University of California
Berkeley, CA 94720, USA

ABSTRACT: Analysis of hydromechanical behavior of fractured rocks requires the use of a numerical method, such as the ROCMAS code developed at LBL (Noorishad *et al.*, 1982). A new numerical technique composed of an incremental recasting of the finite element matrix formulation of the hydroelasticity algorithms, coupled with a modified Newton-Raphson linearization scheme, is developed for such analysis. The resulting code, which we named ROCMAS II, was partially verified using existing solutions in the literature. Complete verification was obtained by cross comparison of the performance of ROCMAS II versus that of its predecessor, the ROCMAS code, since the solution techniques of these two codes are completely different.

The verified ROCMAS II with its major improvements, such as an incremental set-up, the strain-softening and dilating shear, and hyperbolic normal closure joint model, and the new linearization scheme, allows more realistic simulations of a host of rock mechanic problems in saturated rocks. Furthermore, the ROCMAS II set-up provides a proper basis upon which procedures for general treatment of various kinds of material non-linearity can be built.

1 INTRODUCTION

The physiochemical environment of geologic systems are host to natural coupled thermal-hydraulic-mechanical-chemical (THMC) events that are taking place at various rates, depending on the nature of the driving energies. Implementation of geotechnical projects can lead to severe alteration of the natural trend of these coupled processes (Tsang, 1987). Assessment of the influence of these various phenomena on the performance of rock structures requires development of realistic conceptual models. The important part of such a model is conceptualization of the physicochemical phenomena and the usage of proper phenomenological solution techniques. Complexity of the multidisciplinary phenomena narrows the choice of these solution techniques to numerical methods. The hydromechanical phenomena in fractured rocks is one area of coupled processes that has not, until recently (Barton, 1986), attracted much attention. The less obvious and indirect way in which this process affects rocks as opposed to soils, and the difficulty of obtaining the required data for its analysis have been the reasons for this apparent neglect. However, as fluid transport in rocks emerges as a critical issue in a number of major problems of current interest such as the selection, design and operation of waste repositories in hard rocks, investigations of coupled hydromechanical phenomena have become essential. Transport of heat by water adds an additional complication requiring thermohydromechanical consideration in rock masses (Tsang, 1987). Such needs call for development of coupled numerical solution techniques. Earlier works (Noorishad *et al.*, 1971; Noorishad *et al.*, 1982) provide a starting point for such studies. In the following we explain our efforts in developing a new computational method for hydrochemical analysis which (1) overcomes some of the shortcomings of its predecessors, such as linear joint model and non-incremental setup, and (2) can easily be enhanced for application to a wider range of geotechnical problems.

2 INCREMENTAL FINITE ELEMENT FORMULATION FOR HYDROELASTICITY

The formulation for a general incremental law can be achieved by two different approaches. A rigorous approach involves recasting of the field equations and initial and boundary conditions of hydroelasticity in rate forms and development of a rate energy statement (Small *et al.*, 1976). However, incremental formulation can also be obtained by simple differentiation of the non-incremental finite element matrix formulation (see Noorishad *et al.*, 1982). Choosing the latter approach we have:

$$\left.\begin{aligned} K_I \frac{\partial U}{\partial t} - L^T \frac{\partial P}{\partial t} &= \frac{\partial F}{\partial t} \\ -L \frac{\partial U}{\partial t} - E \frac{\partial P}{\partial t} - H_I P &= Q \end{aligned}\right\} \quad (1)$$

where,

K_I = Incremental stiffness matrix
H_I = Incremental conductance matrix
L = coupling matrix
L^T = transpose of L matrix
F = nodal force vector
E = fluid storativity vector
Q = flow vector
U = displacement vector
P = pressure vector

Equation (1) is then integrated between t_1 and $t_2 = t_1 + \Delta t$ to obtain:

$$\begin{aligned} &\overline{K}_I (U_2 - U_1) - L^T (P_2 - P_1) = F_2 - F_1 \\ &-L(U_2 - U_1) - E(P_2 - P_1) - \Delta t \overline{H}_I \overline{P} = \Delta t\, Q(t) \end{aligned} \quad (2)$$

where,

$$\overline{P} = \alpha P_2 + (1-\alpha) P_1 \quad (3)$$

and $\overline{H}_I$ and $\overline{K}_I$ are values of H_I and K_I evaluated at $t = ½(t_1 + t_2)$, $U = ½(U_1 + U_2)$, and $P = ½(P_1 + P_2)$.

In Eq. (3), α is the integration rule parameter with a value between 0 to 1. In final form,

$$\begin{bmatrix} \overline{K}_I & -L^T \\ -L & -E - \alpha \Delta t \overline{H}_I \end{bmatrix} \begin{Bmatrix} \Delta U^i \\ \Delta P^i \end{Bmatrix} = \begin{Bmatrix} \Delta F^i \\ \overline{H}_I \Delta t\, p^{i-1} + Q \Delta t \end{Bmatrix} \quad (4)$$

where,

$$p^{i-1}\big|_{i=1} = \begin{cases} P_0 & \text{current level} \\ 0 & \text{excess level} \end{cases}$$

The solution is expressed in the form of:

$$U^i = U^{i-1} + \Delta U^i$$

$$P_i = P^{i-1} + \Delta P^i$$

The time-march solution technique for linear hydroelasticity is unconditionally stable for values of $\alpha \geq 1/2$ (Booker and Small, 1975). The equations just developed can be strongly nonlinear even though they represent the hydromechanical behavior at an incremental level. The solution to these equations can therefore be obtained either by direct iteration or by one of the Newton-Raphson schemes. The direct method (variable stiffness method), though proven to be a very powerful technique, has at least two disadvantages:

1. The need for an update of the global stiffness matrix at each iteration.
2. The creation of unrealistic conditions for unloading.

Furthermore, strain-softening modeling may be difficult to achieve with the direct iteration method. Modified Newton-Raphson method, on the other hand, offers a better alternative, though, at the expense of slower convergence rate. However, it may be possible to use this technique through the time domain. Critical nonlinear conditions, as well as demands for faster convergence call for updating the stiffness matrices at various time periods. The latter method will be referred to as mixed Newton-Raphson method. We should point out that conditions of large unloading and strain-softening may limit the application of this method. We first implemented the mixed method for ROCMAS II. Within this strategy we have then created an option for solution with the direct iteration method. This means that ROCMAS II has multiple linearization capacity. The stiffness perturbation scheme alone, along with the improved joint model and incremental loading, make ROCMAS II superior to ROCMAS. In the next section we shall show a brief development for the derivation of incremental algorithm for the modified Newton-Raphson method.

3 NEWTON-RAPHSON LINEARIZATION

Equation (4) can be written in a more compact form as:

$$\psi^i(x) = \underline{K}\, \delta x^i - R^i = 0 \quad (5)$$

for departure from an established equilibrium at $i-1$ time level if we assume

$$\delta x_0^i = 0 \rightarrow \psi_0^i = -R^i$$

leads to

$$\delta x_1^i = \underline{K}^{-1}\psi_0^i$$

and,

$$\delta x_j^i = -\underline{K}^{-1}\psi_{j-1}^i$$

therefore,

$$x^i = \Sigma\,\delta x_j^i$$

where,

$$x^i = \begin{Bmatrix} \Delta U^i \\ \Delta P^i \end{Bmatrix}.$$

If we replace the $\overline{K}_I$ and $\overline{H}_I$ in the global stiffness matrix $\underline{K}$ above (i.e., in its expanded form, Eq. (4)) by K_E and H_E, the initial matrices, we arrive at the modified Newton-Raphson algorithm. Writing the above expressions in terms of parameters of Eq. (4) we get,

$$\psi_0^i = \begin{Bmatrix} \Delta F^i \\ \Delta t\,\overline{H}_I P^{i-1} + Q\Delta t \end{Bmatrix} \quad (6)$$

and,

$$\psi_{j-1}^i = \begin{Bmatrix} (\overline{K}_{I_{j-1}}^i - K_E)\delta\Delta U_{j-1}^i \\ \\ -\alpha\Delta t(\overline{H}_{I_{j-1}}^i - H_E)\delta\Delta P_{j-1}^i \end{Bmatrix} \quad (7)$$

and

$$P^i = P^{i-1} + \Delta P^i = P^{i-1} + \sum_{j=1} \delta\Delta P_j^i$$

$$U^i = U^{i-1} + \Delta U^i = U^{i-1} + \sum_{j=1} \delta\Delta U_j^i$$

Index i indicates the time level (i). The above procedure is repeated to arrive at the next time level $(i+1)$. In the mixed method in ROCMAS II, we update the $\underline{K}$ matrix at the beginning of each time level and keep it constant throughout the rest of the iteration in that time level.

4 NONLINEAR MATERIAL MODELS

Although the mechanisms are in place for the implementation of general inelasticity for the continuum in the present work, we have turned to address the nonlinear behavior of fractures in rocks. This is because of the greater and more sensitive role fractures play in the hydroelasticity of rock masses. The joint in the new code has strain-softening shear behavior with a peak shear based on the Ladanyi and Archembault (1970) criterion. The closure behavior follows a hyperbolic compression curve (Goodman, 1975). The new shear model also allows for dilation during shear movement of the joints. This important option allows more realistic determination of fracture apertures, and hence rock permeability in the hydromechanical simulations.

5 VERIFICATION ATTEMPTS

Verification of a coupled code involves systematic verification at the levels of uncoupled single and coupled multiple phenomena. Details of the comprehensive verification can be found in Noorishad and Tsang (1989). In this paper we shall describe a verification study of the fully coupled code. In calculations with the coupled code, care should be taken to ensure strategic refinement of the solution domain, since it is essential to give sufficient details to regions of high gradients that may arise in the system response. This turns out to be of critical importance to the solution stability in nonlinear hydromechanical problems.

In this attempt the aim was to test the performance of ROCMAS II analysis of coupled hydromechanical phenomena in a saturated geological system which is perturbed by both mechanical and hydraulic forces. The motivation is provided by the geomechanical and hydrological setting in a number of underground constructions in saturated rocks. We decided on a scoping model study of a hypothetical tunnel excavation in granitic rocks at a depth of about 300 m. To keep the system at a practical level of computing cost and complexity, we only allowed two major discontinuities to intersect the tunnel, and modeled a quarter of the system. Although this is unrealistic to some degree, the exercise is sufficient for code verification where we need to ensure that the problem fully engages all of the algorithms. The cross section of the tunnel was initially assumed to be rectangular mainly for ease of manual mesh generation. However, after the first few runs it is found that a very high degree of spatial refinement is required near the tunnel. Then a circular cross section which allows for easier automatic mesh generation was used. Figure 1 shows the model schematics and Table 1 enumerates various data used in the simulations. Since the tunnel face is the location of diffusion front—which is at least true for uncoupled fluid flow to the tunnel—a geometric mesh refinement from external boundaries toward the tunnel is necessary. The designed finite element mesh has 503 nodal points and 465 elements for the quarter section of the model. Inside the tunnel, the criterion for mesh design is assumed to be the excavation sequence in a ten-bench excavation procedure. This assumption causes some loss of accuracy and may have created certain numerical problems very early in the solution, mostly in the immediate neighborhood of the unexcavated elements. However, in sequential excavations this problem is found not to be of significance. Considering the effectiveness of direct iteration method (DIR) in addressing nonlinearity, we first solved the problem with the ROCMAS approach of stiffness perturbation. Figure 2 demonstrates the early time evolution of the pressure profile in the fracture. The propagation and attenuation of the high pressures, created due to almost instantaneous loading as excavation is started, follow our expectations. The important point in this behavior is the development of pressures with magnitudes approximately four times the value of the in-situ fluid pressure. These effects can have significant physical implications. However, one aspect of the observed phenomenon that came out of the calculations, is the unexpected variations of the apertures during the development of the pressure profile. In Fig. 3 these variations are plotted for the first element of the vertical and the horizontal fracture neighboring the tunnel. Full closure and significant recovery of the aperture, in the case of the vertical fracture, is very interesting. Bundling of stress trajectories behind and in front of the pressure front and their later separation may be the cause of this phenomena. The horizontal fracture does not experience any significant deformation until the removal of the last bench in the excavation sequence, when the reduction of fluid pressure to the atmospheric level causes some increase in the effective stress and thus slight closure of the fracture. Later-time results show rebounding and widening of this fracture above its initial value before excavation.

Intuitive analysis of the results of the direct iteration solution confirms that a reasonably satisfactory solution had been obtained. Next the ROCMAS II methodology of the mixed Newton-Raphson was employed to solve the same problem. Figure (4) shows the results of this attempt. Dashed lines on the same figure reproduce some of the steps of the direct iteration method for comparison. Considering the strong nonlinearity of the system in the presence of large pressures (developed as a result of the early response of the undrained fractures) and the use of rather coarse discretization with mixed quadrilateral and triangular elements, the comparison is very satisfactory. The stable oscillations of solution can be damped and improved matching can be achieved with more refined and coherent discretization, increased iterations, and by use of further damping. It is worth noting that in order to get this solution we had to replace the algorithm of Eq. (3) with a damped trapezoidal time integration form. With the shortcomings of the discretization and the existing nonlinearity, application of the trapezoidal time integration is required. Considering the fundamental differences of the two linearization schemes that were used in obtaining the two solutions, we are satisfied with the performances of ROCMAS II and ROCMAS, and consider that verification of these codes has been achieved.

6 CONCLUSION

Limitations of the numerical hydroelasticity technique in our ROCMAS code and the lack of availability of other solution methods for nonlinear problems in this area motivated us to develop an alternative numerical technique which not only serves for cross comparison verification purposes, but also possesses additional capabilities and a more suitable basis for further expansions. A brief account of the fundamentals of such a method in the code ROCMAS II is reported. The basic difference between ROCMAS II and its predecessor ROCMAS, lies in the linearization techniques used. ROCMAS employs direct iteration while ROCMAS II uses mixed Newton-Raphson linearization. This fundamental difference provided the possibility of cross verification between the two codes for their hydromechanical nonlinearity handling capability. For this purpose we solved a deep tunnel excavation problem in a hypothetical setting in saturated fractured rock, with the two methodologies and obtained very similar results. This is an important step in giving us confidence that they perform properly as hydromechanical analysis tools. The new code ROCMAS II has options for both linearization techniques and embodies a host of improvements beyond ROCMAS code such as a more realistic joint model and a flexible solution strategy. The incremental set up of the code allows for straightforward implementation of various material nonlinearity models, such as plasticity which are of importance in the rock mechanic investigations of saturated rock environments.

7 ACKNOWLEDGEMENTS

This work is jointly supported by a grant from the Swedish Nuclear Power Inspectorate (SKI), Stockholm, Sweden and by Office of Energy Research, Office of Basic Energy Sciences, Engineering and Geoscience Division of the U.S. Department of Energy through contract number DE-AC03-76SF0098. Discussions and encouragements from Kjell Andersson, Ove Stefansson, Johan Andersson and Alf Larsson are gratefully acknowledged.

REFERENCES

Barton, N. R., 1986. Deformation phenomena in jointed rock, *Geotechnique, 36*, no. 2, 147–167.

Booker, J. R. and Small, J. C., 1975. An investigation of the stability of numerical solutions of Biot's equations of consolidation, *International Journal of Solids and Structures, 11*, 907–917.

Goodman, R. E., 1975. *Methods of Geological Engineering*, West Publishing Co., New York.

Ladanyi, B. and Archambault, G. (1970). Simulation of the shear behavior of a jointed rock mass, *Proc. 11th Symposium on Rock Mechanics (AIME)*, 105–125.

Noorishad, J., Witherspoon, P. A. and Brecke, T. L., 1971. A method for coupled stress and flow analysis of fractured rock masses, *Geotechnical Engineering Publication No. 71-6*, University of California, Berkeley.

Noorishad, J., Ayatollahi, M. S. and Witherspoon, P. A., 1982. Coupled stress and fluid flow analysis of fractured rocks, *International Journal of Rock Mechanics and Mining Sciences, 19*, 185–193.

Noorishad and J. Tsang, C. F., 1989. Recent enhancements of the coupled hydromechanical code: ROCMAS II, *Swedish Nuclear Power Inspectorale*, SKI # TR 89:4.

Small, J. C., Booker, J. R., and Davis, E. H., 1976. Elasto-plastic consolidation of soils, *International Journal of Solids and Structures, 12*, 431–448.

Tsang, C. F., 1987. Coupled processes associated with a nuclear waste repository, Editor. *Academic Press*, San Diego, U.S.A.

Table 1. Material Properties Used for Various Trial Runs with ROCMAS

Material	Property	Value
	Mass Density, ρ_l	1×10^3 kg/m^3
Fluid	Compressibility, β_p	5.13×10^{-1} GPa^{-1}
	Dynamic viscosity, n_l	1×10^{-3} N–sec/m^2
	Young's modulus, E_s	69.0 GPa
	Poisson's ratio, v_s	0.25
	Mass density, ρ_s	2.3×10^3 kg/m^3
Rock	Porosity, ε	0.15
	Intrinsic Permeability, k	10^{-18} m^2
	Biot's constant, M	130 GPa
	Biot's constant, α	1.0
	Initial normal stiffness, K_n	3.7×10^{10} N/m^3 for vertical fracture 1.4×10^{10} N/m^3 for horizontal fracture
	Initial tangential stiffness, K_s	1.2×10^9 Pa/m
	Initial aperture, 26	1×10^{-3} m
	Wall rock compressive strength,* q_u	1×10^3 GPa
	Ratio of tensile to compressive strength,* T_o/q_u	0.1
	Ratio of residual to peak shear,* τ_p/T_r	1.0
	Maximum normal closure,* Vmc	0.014 m
Fractures	Seating load,* ξ	-1×10^4 N/m^2
	Initial dilation angle,* i_o	0
	Friction angle, δ	30°
	Porosity, ε	1.0
	Biot's constant, M	94 GPa
	Biot's constant, α	1.0, 0.0

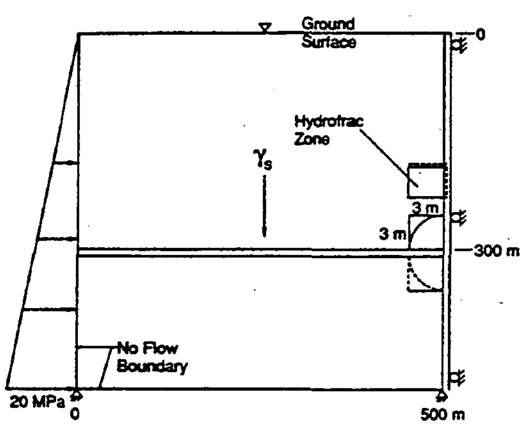

Figure 1. Schematic of the tunnel model.

Number of Elements 503
Number of Nodal Points 465
Hard Rock Data
Medium Permeability

XBL 883-10151

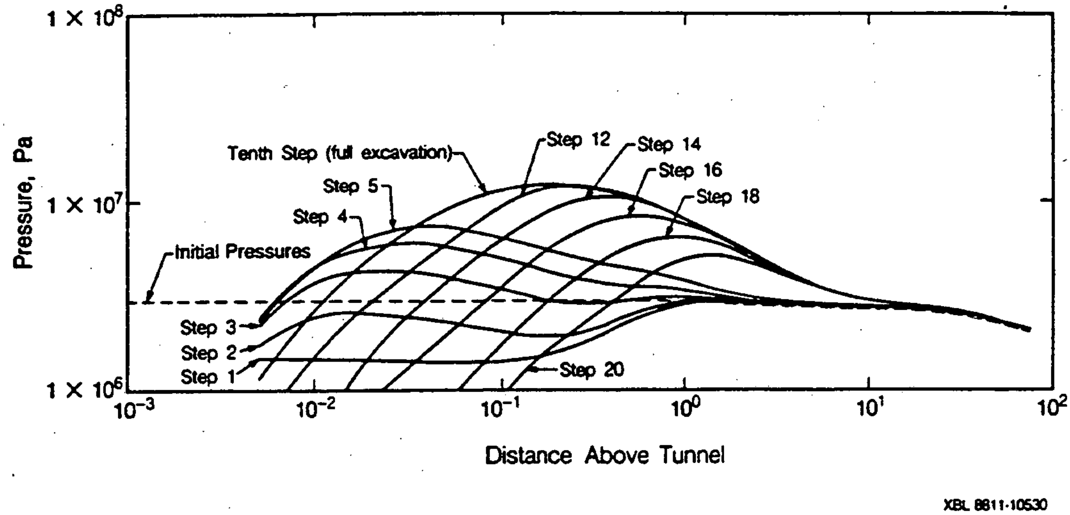

Figure 2. Evolution of the pressure profile inside the vertical fracture during and after excavation.

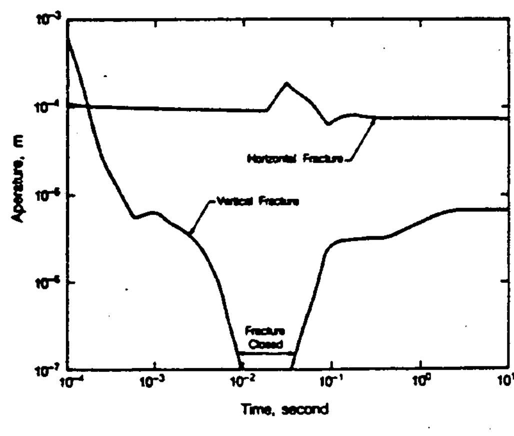

Figure 3. Time variations of the aperture of the vertical and horizontal fractures at the tunnel during and after excavation.

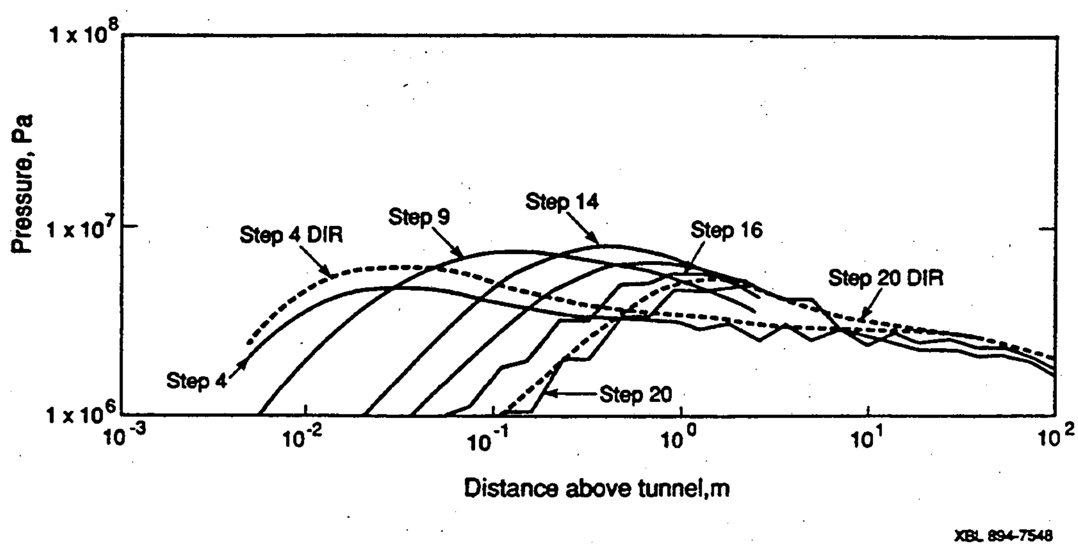

Figure 4. Comparison of pressure profiles in the vertical fracture obtained by ROCMAS and ROCMAS II methodologies. Step numbers above 10 refer to post excavation times.